ADVANCED HEALTHCARE MATERIALS
www.advhealthmat.de

Controlling C2C12 Cytotoxicity on Liquid Metal Embedded Elastomer (LMEE)

*Phillip Won, Stephen Coyle, Seung Hwan Ko, David Quinn, K. Jimmy Hsia, Philip LeDuc, and Carmel Majidi**

Liquid metal embedded elastomers (LMEEs) are highly stretchable composites comprising microscopic droplets of eutectic gallium-indium (EGaIn) liquid metal embedded in a soft rubber matrix. They have a unique combination of mechanical, electrical, and thermal properties that make them attractive for potential applications in flexible electronics, thermal management, wearable computing, and soft robotics. However, the use of LMEEs in direct contact with human tissue or organs requires an understanding of their biocompatibility and cell cytotoxicity. In this study, the cytotoxicity of C2C12 cells in contact with LMEE composites composed of EGaIn droplets embedded with a polydimethylsiloxane (PDMS) matrix is investigated. In particular, the influence of EGaIn volume ratio and shear mixing time during synthesis on cell proliferation and viability is examined. The special case of electrically-conductive LMEE composites in which a percolating network of EGaIn droplets is created through "mechanical sintering" is also examined. This study in C2C12 cytotoxicity represents a first step in determining whether LMEE is safe for use in implantable biomedical devices and biohybrid systems.

1. Introduction

Liquid metal embedded elastomers (LMEEs) have garnered interest in recent years as soft and highly stretchable composites that exhibit a unique combination of mechanical, electrical, and thermal properties.[1–7] LMEEs are rubbery composites composed of a high concentration of microscale liquid metal droplets, typically an eutectic gallium-indium (EGaIn) alloy, suspended within a soft elastomer matrix such as silicone or polyurethane rubber. The elastomer component of the composite allows for LMEEs to undergo high levels of strain while retaining the encapsulated liquid metal. Because they can be engineered to have high thermal conductivity and electrical permittivity while retaining their rubbery elastic properties, LMEE composites have attracted growing attention and have the potential for transformative impact in wearable computing, soft robotics, thermal management, and advanced healthcare applications.[2,4,8–10] However, although promising, little is known about the cytotoxicity of LMEEs and their safety for applications that require direct contact with living cells, tissue, and organs.

A critical factor in the viability and growth of cells cultured of LMEEs is the presence of large concentrations of Ga-based liquid metal alloys. EGaIn, which has a melting point of 15.5 °C, is an especially common material for LMEEs.[3] Composites with an EGaIn volume fraction of >50% can be engineered to exhibit high electrical conductivity ($\sigma = 3.4 \times 10^6$ S m^{-1})[11] using a variety of different elastomer matrix materials.[1,12–20] LMEEs can be synthesized by shear mixing EGaIn into a liquid-phase

P. Won, S. Coyle, D. Quinn
Mechanical Engineering
Carnegie Mellon University
Pittsburgh, PA 15213, USA
S. H. Ko
Mechanical Engineering
Seoul National University
Seoul 08826, Republic of Korea
K. J. Hsia
Chemical & Biomedical Engineering
Nanyang Technical University
Singapore 639798, Singapore
K. J. Hsia
Mechanical & Aerospace Engineering
Nanyang Technical University
Singapore 639798, Singapore
P. LeDuc, C. Majidi
Biomedical Engineering
Carnegie Mellon University
Pittsburgh, PA 15213, USA
E-mail: cmajidi@andrew.cmu.edu
P. LeDuc, C. Majidi
Mechanical Engineering
Carnegie Mellon University
Pittsburgh, PA 15213, USA

The ORCID identification number(s) for the author(s) of this article can be found under https://doi.org/10.1002/adhm.202202430

DOI: 10.1002/adhm.202202430

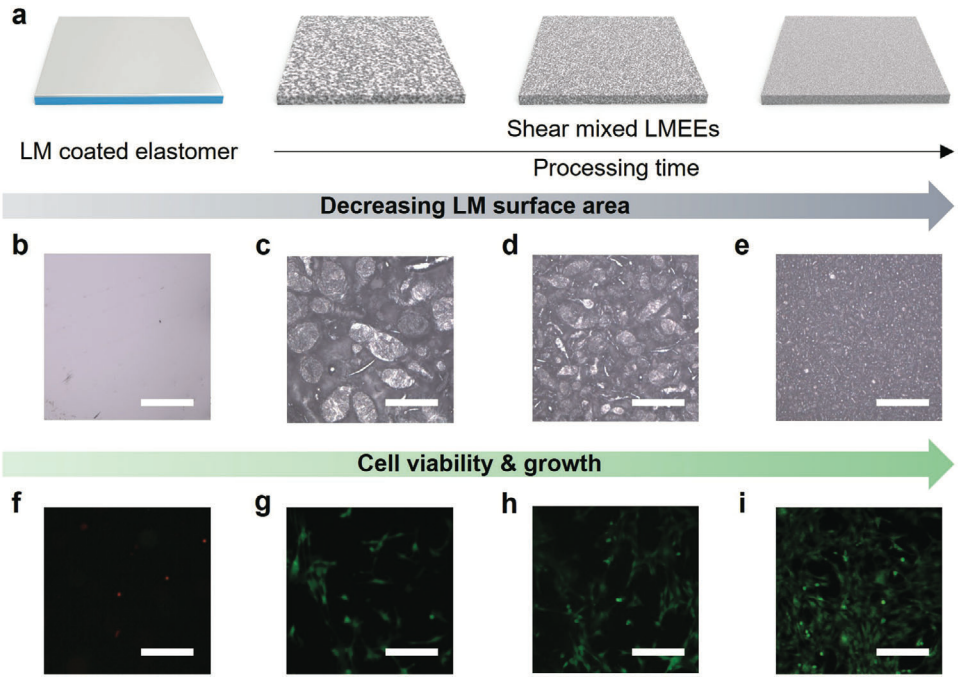

Figure 1. Cytotoxicity of C2C12 mouse myoblast cells cultured on Liquid Metal Embedded Elastomers. a) Illustration of how increasing LMEE shear mixing time corresponds to a decrease in surface exposure of EGaIn liquid metal (LM). Subsequent subfigures correspond to an LM-coated PDMS substrate and LMEE (LM vol 60%; PDMS matrix) composites that are produced by shear mixing for 30 s, 1 min, and 10 min. b–e) Corresponding optical microscope (OM) images showing the different degrees of EGaIn surface coverage. f–i) Examining viability through florescence microscope images of live (green) and dead (red) C2C12 skeletal muscle cells cultured on different LM electrodes. (Scale bars are 200 μm)

elastomer prepolymer. Fabrication through shear mixing relies on the liquid phase of EGaIn and its ability to disperse into droplets that form a gallium oxide skin, which functions as a surfactant.[21] Although it has been speculated that gallium-based alloys are biocompatible, there is evidence that EGaIn can be toxic to cells after ion releases of Ga^+ and In^+ in an aqueous environment when EGaIn is mechanically agitated or sonicated.[22] Thus, EGaIn could become cytotoxic depending on its form (e.g., bulk liquid, microscale droplet, nanoparticle) or exposure conditions, such as mechanical agitation or long incubation time with cells. However, when fully encapsulated as microscale droplets within a soft elastomer matrix, we postulate that EGaIn may no longer pose a source of cytotoxicity, suggesting that LMEEs may have the potential to be biocompatible.

In this study, we investigate the growth and viability of mouse skeletal muscle cells (C2C12 cells) cultured directly on LMEE substrates. In particular, we examine the influence of EGaIn volume fraction, droplet size, and connectivity (i.e., isolated droplets vs connected percolating networks) on C2C12 cytotoxicity. This includes studying how shear mixing conditions (e.g., speed and mixing duration) impact the EGaIn droplet size and distribution. Our findings suggest that the degree of cytotoxicity can be controlled by LMEE composite microstructure and the extent to which EGaIn droplets are fully encapsulated within the elastomer matrix. This study specifically examines the cell culture viability and growth of the C2C12 mouse myoblast cell line with LMEE in which polydimethylsiloxane (PDMS) is used as the elastic matrix material. While there are already many studies that demonstrate high cell viability, growth, and integrability between C2C12 cells and PDMS,[23–27] little is known about C2C12 cellular responses to EGaIn, and, to the best of our knowledge, there is no information regarding their interaction with PDMS-based LMEEs. This work represents the first step in assessing the potential use of LMEE composites for applications that require direct contact with biological cells and tissue.

2. Results & Discussion

2.1. Liquid Metal Surface Area and Cell Viability on LMEE

Cell viability and confluency are important considerations when determining the cytotoxicity of materials.[28–31] In addition, when considering cytotoxicity here, the volume ratio and processing time of LMEEs are important as well. We observed evidence of a direct correlation between liquid metal (LM) surface area and cell viability when cells were cultured on an LMEE surface (**Figure 1**). For LMEEs fabricated with different shear mixing times (which influenced the particles of LM droplets) the exposure of LM surface within LMEE composites at the contact surface decreased with decreasing droplet sizes. The exposed LM surface area decreased with the integration of EGaIn into precured polymers which appeared primarily related to processing (mixing) time. Scanning electron microscope (SEM) images of the surface of LMEE showed that, as the processing time increased, the exposed LM surface area on the outside surface of LMEE decreased considerably (**Figure 2**a–d). This is likely due to the fact that, as processing time increased, the EGaIn became more embedded within and diffused throughout the polymer.

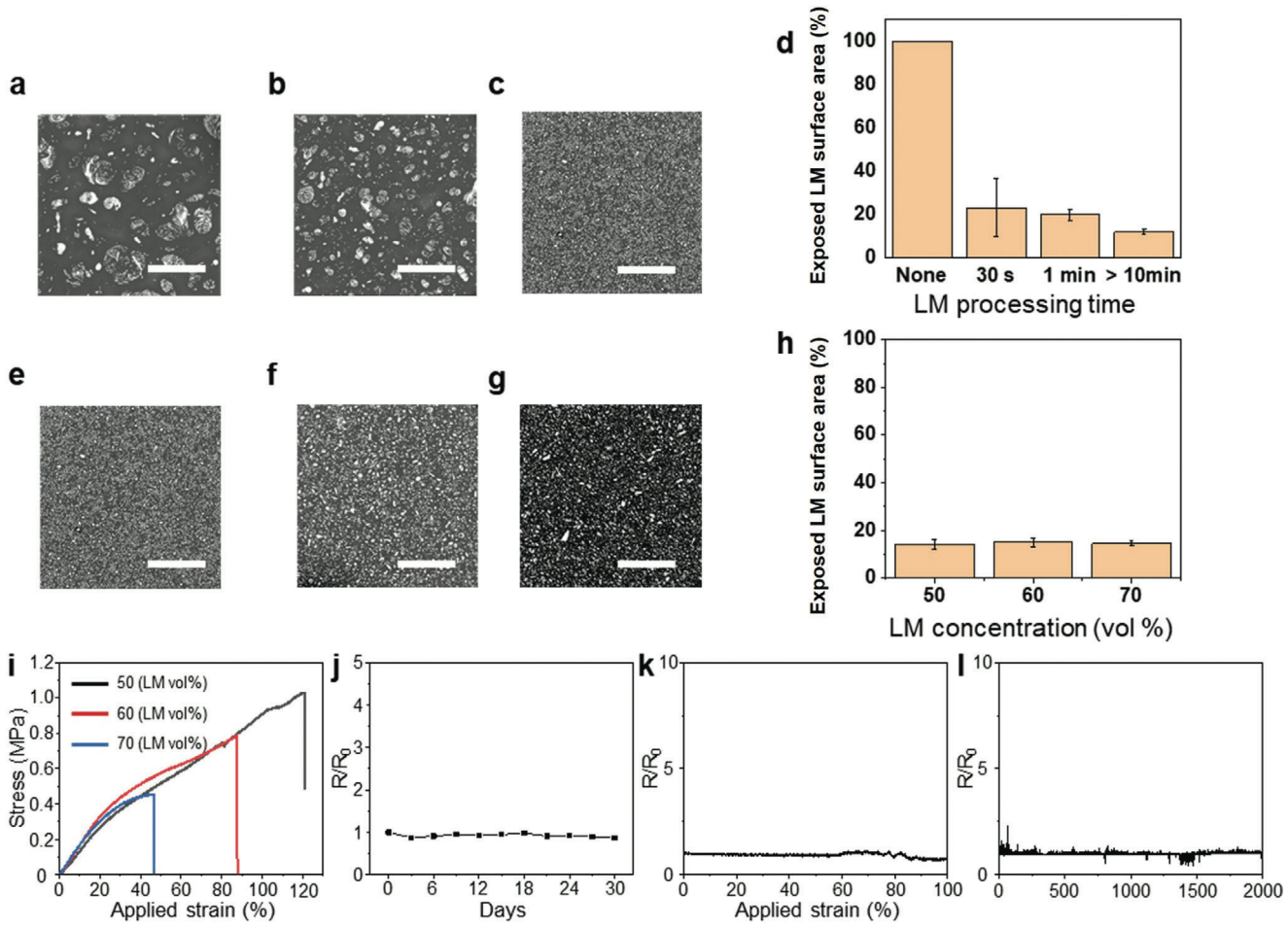

Figure 2. EGaIn surface area measurements. a–c) SEM images of LMEE surfaces with different processing times: (a) 30s, (b) 1 min, and (c) > 10 min. d) The exposed LM surface area (%) measurements with different processing times. e–g) SEM images of LMEE surfaces with different LM volume concentrations. h) The exposed LM surface area (%) measurements with different LM volume concentrations. i–l) Characterization of LMEE electrodes. (i) Stress-strain curves of LMEE with different LM concentrations, (j) Oxidation stability test with a change in resistance of 15 mm x 15 mm LMEE (LM vol 60%) electrode over time in a water bath for 30 days. (k, l) Electrical properties of LMEE under deformations (LM vol 60%, stretching area – 30 mm x 10 mm), (k) relative resistance under applied strains, and (l) relative resistance under cyclic stretching (strain of 50%). Note that the LM volume is fixed at 60% for (j–l). (sample size n = 5, all bar charts present mean ± standard deviation)

Additionally, the release of cytotoxic ions at the surface of LMEE was expected to be lower with smaller EGaIn droplets due to lower liquid metal area at the surface and increased EGaIn confinement within LMEE architecture.[22,32] The increase in surface area of the biocompatible polymer and decrease in droplet size were correlated to an increase in cell viability and growth when cultured on the LMEE (Figure 1b–j). The correlation to increased cell viability and growth to PDMS surface area is likely due to the role that the commonly used extracellular matrix (ECM), fibronectin, plays in promoting cell adhesion. PDMS used for cell culture is often coated with ECM proteins.[33] The coating occurs because of a physical, weak bonding between PDMS and ECM proteins Fibronectin promotes cell adhesion via interactions between itself and cell surface receptors such as integrins.[34]

The exposed LM surface area was minimized after at least 10 min of mixing. Furthermore, processing times of at least 10 min minimized the exposed LM surface area on the outside of the LMEE, irrespective of volume ratio differences. Although there were considerable differences in the total EGaIn between 50%, 60%, and 70% volume concentrations, the exposed LM surface area percentages were all equal after at least 10-min processing times (Figure 2e–h). LM volume concentrations above 70% were not investigated as there would not be enough PDMS to encapsulate EGaIn droplets and LM; this would compromise the integrity of LMEE structure and increase the LM surface area on the LMEE surface.

2.2. Characterization of LMEE

The material properties of LMEE at different volume concentrations were compared to understand the potential tradeoffs between cytotoxicity and material performance. The stretchability of LMEE decreased with higher volumetric contents of LM (Figure 2i). The moduli of each concentration were consistent as they ranged from 700 to 800 kPa in lower strain (< 30%). For the

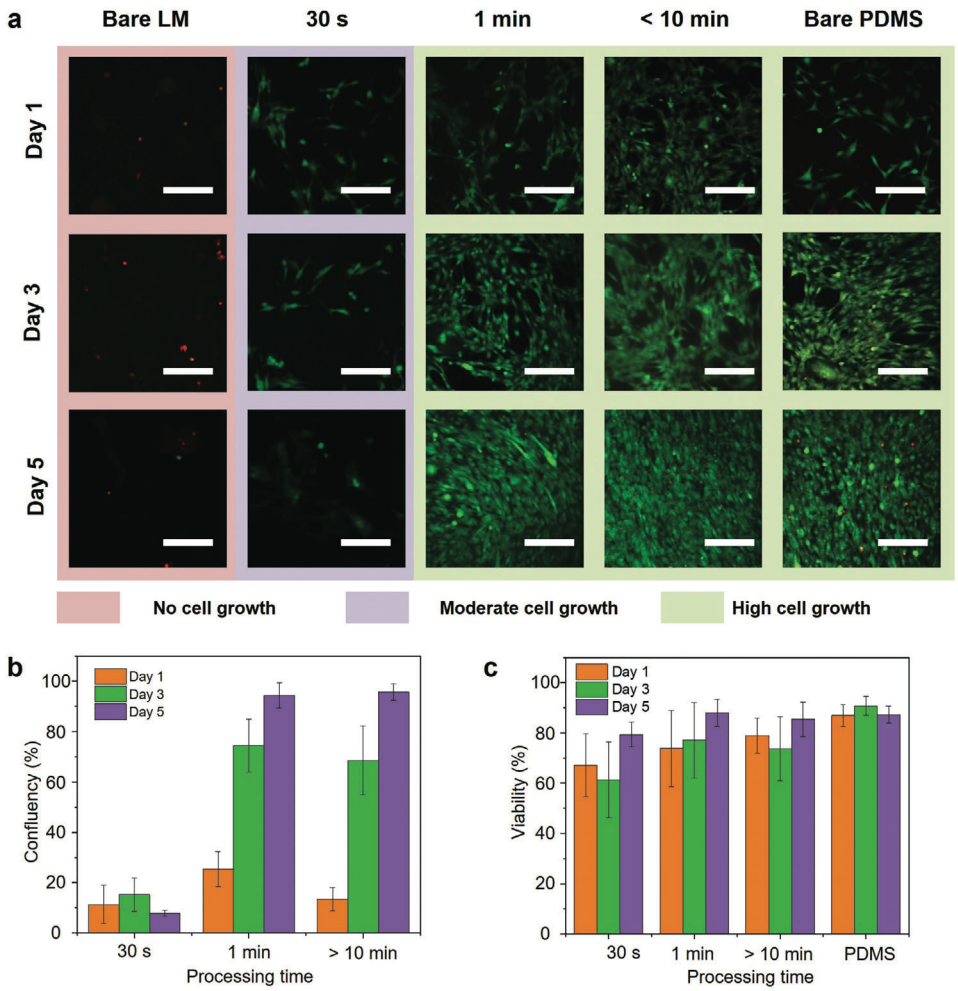

Figure 3. Cytotoxicity tests for LMEE for LM processing and integration. a) Fluorescence images of live (green) and dead (red) cells on LMEE with different conditions; Bare LM on a PDMS substrate, LMEE with different shear mixing times, and a bare PDMS substrate. b) Cell confluency after multi-day proliferation of C2C12 cells, measured for 1, 3, and 5 days. c) Cell viability on LMEE for 1, 3, and 5 days. (c, d sample size n = 9, all bar charts present mean ± standard deviation)

electrical conductivity experiments, the 60% volume of LMEE was utilized for the biohybrid device due to its moderate stretchability, electrical conductivity, cell viability, and cell growth. To examine the electrical stability in aqueous conditions, where the environment is suitable for cell culture, the LMEE samples were tested for 30 days and negligible change in electrical resistance was found after 30 days (Figure 2j). Likely due to the unique mechanical coupling behavior of LMEE,[12–13,35] which can have a great advantage over other soft electrical conductors, a plateau in the increase in electrical resistance was found for applied strains of up to 100% (Figure 2k). Moreover, the LMEE sample was stretched up to 50% applied strain repetitively to demonstrate electromechanical stability under cyclic strains (Figure 2l).

2.3. Cell Viability and Confluency on LMEE

When culturing cells on LMEE, shear mixing time (**Figure 3**) and volume ratio of LMEE (50%, 60%, and 70%; **Figure 4**) appeared to be the most important variables for low cytotoxicity. There was substantially improved cell viability and confluency on surfaces that had a processing time of 1 min or longer, and an inverse relationship between the volume ratio of EGaIn to PDMS, and cell viability and confluency. An LMEE with volume ratio of 60% and processing time of 10 min is optimal because viability and confluency were similar to PDMS. C2C12 cells were cultured for 5 days on EGaIn-PDMS LMEE at different percent volume ratios (50%, 60%, and 70%) to compare cell confluency and viability. Although cell viability was the highest for LMEE of 50% volume ratio, its conductivity was the lowest, which means that such composites can still exhibit enhanced thermal conductivity and electrical permittivity but are likely not well suited for applications that require electrical conductivity.

For LMEE composites with high EGaIn concentrations (i.e., 60% vol fraction), electrical conductivity can be induced by stretching to a 30% strain (**Figure 5**). As had been previously reported in the literature, mechanical loading causes EGaIn droplets to rupture and coalesce to form conductive

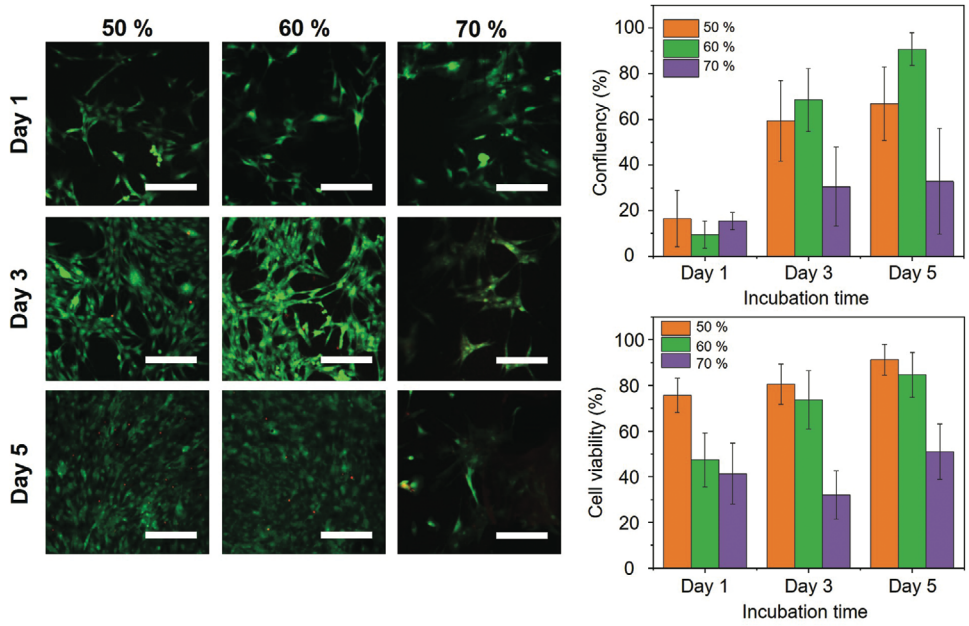

Figure 4. Cytotoxicity tests for LMEE related to LM concentration (vol %). a) Fluorescence images of live (green) and dead (red) cells on LMEE with controlled volume ratios: 50%, 60%, and 70% volume ratios. b) Cell confluency after multi-day culture of C2C12 cells, measured for 1, 3, and 5 days. c) Cell viability on LMEE for 1, 3, and 5 days. Scale bar 200 µm. (sample size n = 9, all bar charts present mean ± standard deviation)

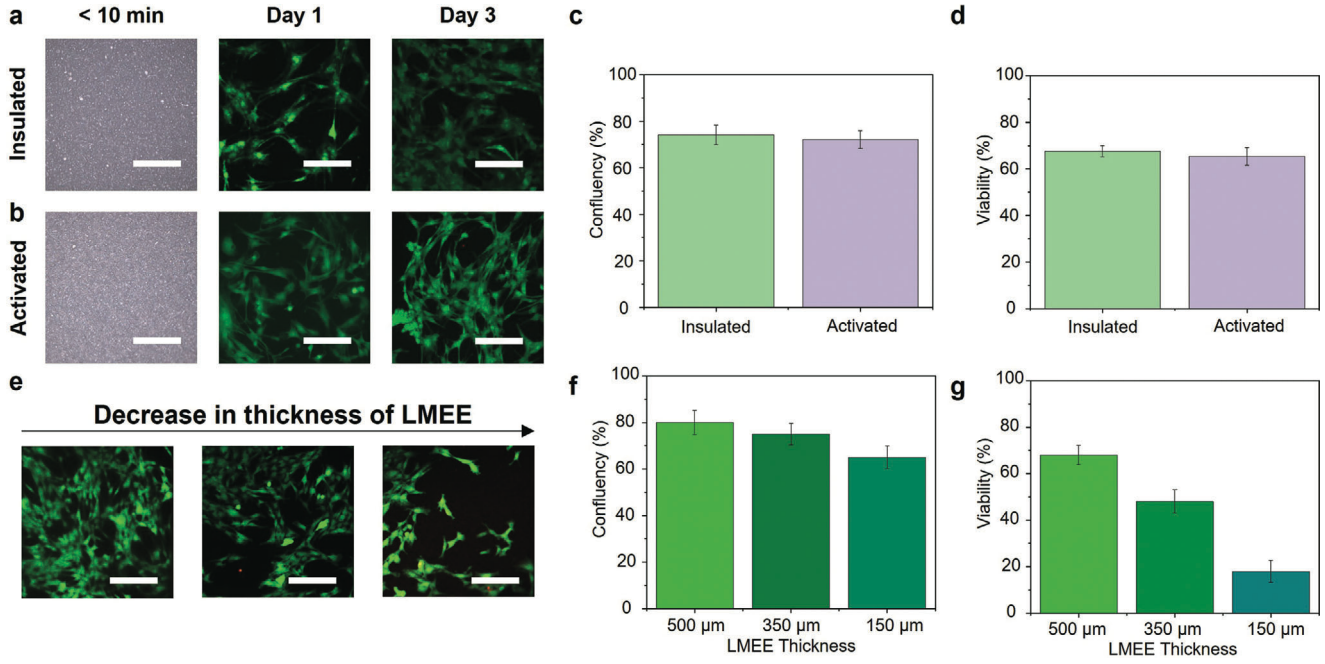

Figure 5. Comparison of insulated and activated LMEE (60 LM vol %) for cytotoxicity. a) Insulated LMEE and b) activated LMEE (left – digital camera image, middle/right – fluorescence images C2C12 cultured Day 1,3) LMEE insulated versus activated data for c) confluency and d) viability. e) Thickness-dependent cell growth data for f) confluency and g) viability on the LMEE (60 LM vol %). (Thickness: left – 500 µm, middle – 350 µm, right – 150 µm). All Scale bars are 200 µm. (sample size n = 9, all bar charts present mean ± standard deviation)

pathways.[36,37] Without this so-called "mechanical sintering" step, the droplets remain isolated from each other and will not form an electrically conductive network. Ford et al., compared the resistance of different volume ratios of LMEE that were activated and found that a 60% volume ratio of LMEE was adequate for achieving low electrical resistance.[13] Referring to Figure 5a,b, we observed that such composites allow for both high electrical conductivity and support high confluency of the cell culture. Moreover, as shown in Figures S2–S6, Supporting Information, we do not see a significant increase in EGaIn exposure when the LMEE

composite is activated through mechanical sintering to achieve electrical conductivity.

As shown in Figure 5c–e, the cell confluency is influenced by the thickness of the LMEE substrate. The fluorescent microscope live/dead cells images with LMEE samples of different thicknesses (referred to as thick, medium, and thin, which had thicknesses of 500, 350, and 150 µm, respectively) showed that the cell confluency consistently decreased with decreasing thickness of fabricated LMEE films. This may be due to the reduced sedimentation of EGaIn microdroplets in thinner samples, resulting in higher concentrations of liquid metal near the cell culture surface.

In addition to studies with Sylgard 184, we also synthesized LMEE composites with Ecoflex as the elastomer matrix material. Ecoflex has been popular as a platinum-cured silicone rubber on account of its low elastic modulus (<100 kPa) and high strain limit (>600%). Similar to the previous studies with Sylgard-based LMEE, cells were cultured on Ecoflex and Ecoflex-based LMEE for 5 days to analyze the differences in viability and confluency (Figure S1, Supporting Information) with different polymer matrixes. Although viability and confluency of cells cultured on Ecoflex were consistently greater than that of the Ecoflex-based LMEE, cell viability and confluency appeared to be high enough on the LMEE for potential biohybrid applications.

3. Conclusions

In this study, we investigated the cytotoxicity of C2C12 cells on silicone-based LMEE substrates engineered with varying liquid metal concentrations and microstructures. Our study revealed that cell viability, when cultured on LMEEs, was highly dependent on EGaIn droplet size, volume fraction, and droplet distribution. Although a study on a wider range of biological cells is required, this investigation suggests that having a controlled volume concentration (as high as 70 LM vol %) and reduced EGaIn droplet size (as small as a few microns in diameter) can potentially allow for better interfacing with natural tissue. Also, the exposed LM surface area decreased with the integration of EGaIn into precured polymers, which appeared to be related to processing time. This is important as previously integrating skeletal muscle tissue with soft materials that are biocompatible and conductive has been challenging.[38–41] Here we observe that LMEE composites with an EGaIn volume fraction of as high as 70% did not show evidence of C2C12 cytotoxicity. Moreover, our measurements with electrically conductive LMEE composites that have 60 vol% of EGaIn also show evidence of high C2C12 viability and growth. Such results do not absolutely prove that LMEE is not cytotoxic, but do represent a first step in showing that LMEE composites could be promising in future healthcare or biohybrid applications that require direct contact with biological cells and tissue. Future LMEE studies, with different cell types and biohybrid applications, should be considered.

4. Experimental Section

Synthesis of Liquid Metal Embedded Elastomer (LMEE): To synthesize eutectic gallium indium (EGaIn), bulk gallium and indium (Ga 75%, In 25% by weight; Rotometals) were placed and heated in a glass vial for 20 h at 200 °C. At the same time, the matrix polymer, polydimethylsiloxane (Sylgard 184; Dow Corning) mixed at a 10:1 base to cross-linker ratio was prepared. EGaIn was added into the uncured prepolymer at the desired volumetric concentration (50%, 60%, or 70%) and mixed using an overhead stirrer (OS20-S, SCILOGEX) at 200 rpm for different time durations. The uncured LMEE composite was then cast in a mold with a thickness of 1 mm for all of the cytotoxicity tests unless otherwise noted. In addition to Sylgard 184, LMEE composites were also fabricated using Ecoflex (Smooth-On) silicone rubber as the matrix material. These Ecoflex-based LMEE composites were fabricated by adding EGaIn into the uncured prepolymer at a desired 60% volumetric concentration and mixed using an overhead stirrer for 10 min (OS20-S, SCILOGEX) at 200 rpm.

Surface Area Measurement: Scanning electron microscope (SEM) images were captured using a desktop SEM (Phenom XL). The SEM images were analyzed using the software, ImageJ, to measure the exposed EGaIn area at the LMEE surface. After collecting the measured surface area, the data was then plotted in a separate data analytic program, OriginPro, for quantitative analysis to observe the effect of cytotoxicity with stirring time and LM volumetric concentrations in LMEE.

Mechanical and Electro-Mechanical Characterization: The LMEE samples were prepared in a dog-bone geometry (ASTM D412) and were tested on a universal testing system (UTS) (5969, Instron) at a strain rate of 5 mm min^{-1} for all tensile testing experiments. The samples were prepared with different EGaIn concentrations for the characterization (50, 60, and 70 LM vol %). For the measurements of electro-mechanical coupling (i.e., change in electrical resistance with stretch) and long-term stability, testing was limited to LMEE samples with a 70% volume fraction of liquid metal. For electro-mechanical characterization, electrical conductivity was induced by rupturing the EGaIn droplets within the matrix to form conductive pathways. This was accomplished under mechanical loading by applying 30% strain using a linear stretcher (A150602-S1.5, Velmex). The electromechanical tests measured the resistance at given strains using a micro-ohm meter (34420A, HP) with a four-point probe. The external analog data from the materials testing machine and voltage signal from the voltage divider circuit were collected using a USB DAQ (USB-6002, NI) with a sampling rate of 300 Hz through the serial interface (MATLAB, 2019a).

Cell Culture for Material Interfaces: PDMS, EGaIn-PDMS, Ecoflex, and EGaIn-Ecoflex samples were sterilized in 70% ethanol and rinsed in deionized water for cell culture. After drying, the samples were plasma oxidized for 60 s at 18 W (PDC-32G) and then coated with 50 µg mL^{-1} of fibronectin (SIGMA) from human plasma for 1 h. Excess fibronectin was aspirated, and then the samples were washed in a phosphate-buffered saline (PBS) bath. Mouse myoblast C2C12 cells (ATCC) were seeded on the patterned side of the PDMS scaffolds at 10 000 cells cm^{-2}. Cells were cultured in growth medium comprised of Dulbecco's Modified Eagle Medium (DMEM, ThermoFisher 11995065) supplemented with 10% Fetal Bovine Serum (ATCC 30–2020) and 1% Penicillin (ATCC 30–2300).

Cell Staining: Fluorescent imaging was conducted at 1, 3, and 5 days after initiating cell seeding using live/dead stains (LIVE/DEAD Viability/Cytotoxicity Kit, Thermofisher). A staining solution of 5 µL calcein AM (Component A) and 20 µL ethidium homodimer-1 (Component B) to 10 mL DPBS was prepared. The culture medium was removed from the cells and replaced with the staining solution directly on the cells. The samples were incubated for 30 min. Since the samples were not opaque, they were inverted onto their top surface and fluorescent images were captured using the CSU-X1.

Cell Viability and Confluency Measurement: Cell viability and confluency of fluorescent images were calculated using the software, ImageJ. The number of live and dead cells in a fluorescent image was calculated by analyzing the number of particles in the red and green channels respectively. Cell viability was calculated by dividing the number of live cells detected by the total number of live and dead cells in an image and multiplied by 100%. Cell confluency, the percent area of cell culture material covered by adherent cells, was calculated using the ImageJ plug-in PHANTAST.[42]

Statistical Analysis: SEM images were captured using a desktop SEM (Phenom XL). The SEM images were analyzed using the software, ImageJ, to measure the exposed EGaIn area at the LMEE surface

(Figure 2 & Figure S6, Supporting Information). After collecting the measured surface area, the data was then plotted in a separate data analytic program, OriginPro, for quantitative analysis to observe the effect of cytotoxicity with stirring time and LM volumetric concentrations in LMEE. Bar charts were of the mean (n = 5) and standard deviation of the % LM surface area. Measurements of resistance of LMEEs were normalized by R_0 (2.2 Ω) in Figure 2j–l.

Cell viability and confluency of fluorescent images were also calculated using the software, ImageJ (Bar charts in Figures 3–5 & Figure S1, Supporting Information). The number of live and dead cells in a fluorescent image was calculated by analyzing the number of particles in the red and green channels, respectively. Cell viability was calculated by dividing the number of live cells detected by the total number of live and dead cells in an image and multiplying by 100%. Cell confluency, the percent area of cell culture material covered by adherent cells, was calculated using the ImageJ plug-in PHANTAST. Bar charts represent the mean (n = 9) and standard deviation of cell viability and cell confluency when cultured on LMEEs.

Supporting Information

Supporting Information is available from the Wiley Online Library or from the author.

Acknowledgements

This work was partially supported by the Air Force Research Lab (AFRL) Nano Bio-Materials Consortium (NBMC) and CMU-Portugal Large-Scale Collaborative Research Projects program.

Conflict of Interest

The authors declare no conflict of interest.

Data Availability Statement

The data that support the findings of this study are available from the corresponding author upon reasonable request.

Keywords

C2C12, cytotoxicity, liquid metal embedded elastomers, skeletal muscles

Received: September 22, 2022
Revised: January 17, 2023
Published online: April 19, 2023

[1] N. Kazem, T. Hellebrekers, C. Majidi, *Adv. Mater.* **2017**, *29*, 1605985.
[2] C. Majidi, K. Alizadeh, Y. Ohm, A. Silva, M. Tavakoli, *Flexible Printed Electron.* **2022**, *7*, 013002.
[3] S. Chen, H.-Z. Wang, R.-Q. Zhao, W. Rao, J. Liu, *Matter* **2020**, *2*, 1446.
[4] M. H. Malakooti, M. R. Bockstaller, K. Matyjaszewski, C. Majidi, *Nanoscale Adv.* **2020**, *2*, 2668.
[5] B. Yao, W. Hong, T. Chen, Z. Han, X. Xu, R. Hu, J. Hao, C. Li, H. Li, S. E. Perini, *Adv. Mater.* **2020**, *32*, 1907499.
[6] S. Liu, S. Y. Kim, K. E. Henry, D. S. Shah, R. Kramer-Bottiglio, *ACS Appl. Mater. Interfaces* **2021**, *13*, 28729.
[7] T. Kim, D.-m. Kim, B. J. Lee, J. Lee, *Sensors* **2019**, *19*, 4250.
[8] L. Mou, J. Qi, L. Tang, R. Dong, Y. Xia, Y. Gao, X. Jiang, *Small* **2020**, *16*, 2005336.
[9] B. M. Li, B. L. Reese, K. Ingram, M. E. Huddleston, M. Jenkins, A. Zaets, M. Reuter, M. W. Grogg, M. T. Nelson, Y. Zhou, *Adv. Healthcare Mater.* **2022**, 2200745.
[10] J. Oh, S. Kim, S. Lee, S. Jeong, S. H. Ko, J. Bae, *Adv. Funct. Mater.* **2021**, *31*, 2007772.
[11] M. D. Dickey, R. C. Chiechi, R. J. Larsen, E. A. Weiss, D. A. Weitz, G. M. Whitesides, *Adv. Funct. Mater.* **2008**, *18*, 1097.
[12] A. Fassler, C. Majidi, *Adv. Mater.* **2015**, *27*, 1928.
[13] M. J. Ford, D. K. Patel, C. Pan, S. Bergbreiter, C. Majidi, *Adv. Mater.* **2020**, *32*, 2002929.
[14] C. Pan, D. Liu, M. J. Ford, C. Majidi, *Adv. Mater.* **2020**, *5*, 2000754.
[15] J.-E. Park, H. S. Kang, J. Baek, T. H. Park, S. Oh, H. Lee, M. Koo, C. Park, *ACS Nano* **2019**, *13*, 9122.
[16] M. Liao, H. Liao, J. Ye, P. Wan, L. Zhang, *ACS Appl. Mater. Interfaces* **2019**, *11*, 47358.
[17] Y. Xin, H. Peng, J. Xu, J. Zhang, *Adv. Funct. Mater.* **2019**, *29*, 1808989.
[18] A. T. Haque, R. Tutika, R. L. Byrum, M. D. Bartlett, *Adv. Funct. Mater.* **2020**, *30*, 2000832.
[19] Y. Xin, Y. Lou, H. Liu, D. Wu, J. Zhang, *Adv. Mater. Technol.* **2021**, *6*, 2000852.
[20] G. Chen, X. Deng, L. Zhu, S. Handschuh-Wang, T. Gan, B. Wang, Q. Wu, H. Fang, N. Ren, X. Zhou, *J. Mater. Chem. A* **2021**, *9*, 10953.
[21] T. Daeneke, K. Khoshmanesh, N. Mahmood, I. A. De Castro, D. Esrafilzadeh, S. Barrow, M. Dickey, K. Kalantar-Zadeh, *Chem. Soc. Rev.* **2018**, *47*, 4073.
[22] J.-H. Kim, S. Kim, J.-H. So, K. Kim, H.-J. Koo, *ACS Appl. Mater. Interfaces* **2018**, *10*, 17448.
[23] S. Coyle, B. Doss, Y. Huo, H. R. Singh, D. Quinn, K. J. Hsia, P. R. LeDuc, *Acta Biomater.* **2022**, *142*, 149.
[24] Y. Sun, R. Duffy, A. Lee, A. W. Feinberg, *Acta Biomater.* **2013**, *9*, 7885.
[25] K. Shimizu, H. Fujita, E. Nagamori, *Biotechnol. Bioeng.* **2009**, *103*, 631.
[26] R. N. Palchesko, L. Zhang, Y. Sun, A. W. Feinberg, *PLoS One* **2012**, *7*, e51499.
[27] D. Sud, G. Mehta, K. Mehta, J. Linderman, S. Takayama, M.-A. Mycek, *J. Biomed. Opt.* **2006**, *11*, 050504.
[28] Z. Wang, H. Kumar, Z. Tian, X. Jin, J. F. Holzman, F. Menard, K. Kim, *ACS Appl. Mater. Interfaces* **2018**, *10*, 26859.
[29] R. Sharifi, S. Mahmoudzadeh, M. M. Islam, D. Koza, C. H. Dohlman, J. Chodosh, M. Gonzalez-Andrades, *Adv. Mater. Interfaces* **2020**, *7*, 1900767.
[30] H. C. Fuller, T.-Y. Wei, M. R. Behrens, W. C. Ruder, *Micromachines* **2020**, *11*, 947.
[31] Z. Y. Jonelle, E. Korkmaz, M. I. Berg, P. R. LeDuc, O. B. Ozdoganlar, *Biomaterials* **2017**, *128*, 109.
[32] T. Cole, K. Khoshmanesh, S.-Y. Tang, *Adv. Intell. Syst.* **2021**, *3*, 2000275.
[33] G. K. Toworfe, R. J. Composto, C. S. Adams, I. M. Shapiro, P. Ducheyne, *J. Biomed. Mater. Res., Part A* **2004**, *71*, 449.
[34] F. Akther, S. B. Yakob, N.-T. Nguyen, H. T. Ta, *Biosensors* **2020**, *10*, 182.
[35] Z. Yu, J. Shang, X. Niu, Y. Liu, G. Liu, P. Dhanapal, Y. Zheng, H. Yang, Y. Wu, Y. Zhou, *Adv. Electron. Mater.* **2018**, *4*, 1800137.
[36] L. Tang, S. Cheng, L. Zhang, H. Mi, L. Mou, S. Yang, Z. Huang, X. Shi, X. Jiang, *iScience* **2018**, *4*, 302.
[37] E. J. Markvicka, M. D. Bartlett, X. Huang, C. Majidi, *Nat. Mater.* **2018**, *17*, 618.
[38] Y. Kim, G. Pagan-Diaz, L. Gapinske, Y. Kim, J. Suh, E. Solomon, J. F. Harris, S. Nam, R. Bashir, *Adv. Healthcare Mater.* **2020**, *9*, 1901137.
[39] S. Li, Y. Cong, J. Fu, *J. Mater. Chem. B* **2021**, *9*, 4423.
[40] D. Gao, K. Parida, P. S. Lee, *Adv. Funct. Mater.* **2020**, *30*, 1907184.
[41] J.-K. Chang, M. B. Emon, C.-S. Li, Q. Yang, H.-P. Chang, Z. Yang, C.-I. Wu, M. T. Saif, J. A. Rogers, *ACS Nano* **2018**, *12*, 9721.
[42] N. Jaccard, L. D. Griffin, A. Keser, R. J. Macown, A. Super, F. S. Veraitch, N. Szita, *Biotechnol. Bioeng.* **2014**, *111*, 504.